Exciton-exciton scattering dynamics in a semiconductor microcavity and stimulated scattering into polaritons

F. Tassone and Y. Yamamoto

ERATO Quantum Fluctuation Project, Ginzton Laboratory, Stanford University, Stanford, California 94305

We study the polariton dynamics in a semiconductor microcavity for small temperatures and zero exciton-cavity detuning, including the exciton-exciton and exciton-phonon scatterings. A bottleneck in the relaxation of excitons into lower polariton is found, which persists up to high densities. We then consider injection of large populations of lower polaritons with an external pump. All scatterings featuring the lower polariton as the final state become stimulated. In particular, scattering of two excitons into both lower and upper polaritons shows direct evidence of stimulation. Within the rate equation approach, we also predict sizable saturation effects due to the stimulated emission. [S0163-1829(99)06615-1]

I. INTRODUCTION

Semiconductor microcavities featuring high-reflectivity dielectric mirrors resulted in the realization of the strong coupling between radiation and matter in two dimensions.[1] This renewed the interest in the exciton-polaritons, also because the signature of strong-coupling, i.e., the splitting of the degenerate exciton and cavity photon modes, is readily observable in emission and reflectivity, in contrast to the bulk polaritons. More generally, the dispersion of the exciton-polaritons is also readily observable by changing the angle of observation.[2] The first studies basically focused on these aspects of the polariton system, and only later their dynamical properties were addressed.[3] Although the cavity photon acquires a mass because of confinement, this is about four orders of magnitude smaller than the typical exciton mass, and strong mixing is only effective in a very small fraction of the k space spanned by thermalized excitons. For larger k vectors, the exciton and photon do not mix and retain their character. In the following, we refer to lower polaritons (LP) and upper polaritons (UP) as the strongly mixed modes close to $k=0$, and to excitons as the unmixed modes at larger k having excitonlike character. Both the LP and UP have a small mass, and density of states (DOS), due to their large photon component. All dynamical properties of the exciton-polariton system are dominated by these two related features, the small fraction of k space occupied by polaritons, and their small DOS. Indeed, the overall relaxation and scattering dynamics of the excitons is negligibly modified by the photon confinement, because a negligible fraction of excitons relax into polaritons.[4] An outstanding prediction is related to the *bosonic* nature of the LP: quasithermal LP at a temperature below half the splitting are strongly degenerate bosons already at small density, due to the small DOS.[5] However, there are serious problems in assuming a thermal distribution of LP. (i) The total phonon scattering into the LP modes is small due to the small final DOS.[5] (ii) As the *radiative* lifetime of polaritons is smaller than the phonon scattering rate, the polariton population remains lower than the thermal population,[6] i.e., a bottleneck in the relaxation of excitons to LP is found. This is analogous to the bulk, where the bottleneck was predicted by Toyozawa,[7] and later observed by many groups.[8] Therefore, the strongly degenerate

bosons at small density were never observed,[9,10] and the observation of the bosonic nature of microcavity polaritons remained questionable. Here we instead show that it becomes relevant in appropriate conditions.

In this paper, we extend the calculations of the dynamics of the exciton-polariton system of Ref. 6 in which only acoustic-phonon scattering was considered, and include exciton-exciton scattering. The interaction between excitons is an effecive mean to take into account the fermionic nature of the exciton constituents, the electron, and the hole, as we will explain later. We treat the exciton-exciton scattering within the rate equation approach also used in Ref. 6. Previous results of unvaried exciton dynamics in the microcavity and existence of a bottleneck in their relaxation to LP are based on the small LP DOS, and short LP lifetimes. They are thus fairly general, and not intimately connected to the nature of the exciton to polariton scattering. These results are here confirmed even at larger exciton densities when exciton-exciton scattering is taken into account.[11] Scattering of excitons into polaritons is a unique feature of strong coupling. We subsequently focus on this dynamic. We identified two qualitatively different types of scattering from a dense exciton reservoir: scattering of two excitons into another exciton and a UP (or LP), or scattering of two excitons into both a UP and a LP. We then consider injection of a finite LP population with an external laser beam. We argue that a large LP population can be produced, because scattering out of the populated state is quenched by the small LP DOS. The scatterings involving the LP as a final state will be stimulated. This is a unique bosonic feature of the system. In particular, the scattering to both UP and LP experimentally allows us to measure the stimulation from the UP emission. Quantitive estimations show that this effect is relevant and observable. Moreover, the stimulated emission of excitons into the LP entails saturation effects at large densities, which is another observable signature of stimulated emission.

The paper is divided as follows. In Sec. II we introduce the bosonic picture of interacting excitons, and report the relevant interaction Hamiltonians. In Sec. III we introduce the rate equation approach, report the exciton-polariton dispersion, radiative recombination rates, for the considered

GaAs based system, and the closed expressions for the exciton-exciton and the exciton-phonon scattering rates. We then discuss the numerical integration of the rate equations, and their physical limits of validity. Finally, we show the stationary solutions in the presence of an exciton pump. In Sec. IV we examine the stimulation effects of the exciton-exciton scattering, when a large LP population is injected with an additional pump. We show that they are relevant, and observable in experiment. In Sec. V we examine saturation effects due to stimulated emission of excitons into LP, and discuss other saturation effects beyond the semiclassical approximation. Finally, we conclude and discuss the relevance of interface disorder on the exciton-polariton dynamics in Sec. VI. The exciton-exciton scattering Hamiltonian is derived with a straightforward procedure in Appendix A, and useful simplified analytical expressions for the exciton to polariton scatterings are given in Appendix B.

II. NONLINEAR INTERACTIONS

In this section we introduce the bosonic exciton picture. Athough widely known, we wish to remark on its relevance and limitations, and its connections to the more fundamental fermionic theory, which involves fermionic excitations of the valence band (holes) and conduction band (electrons), and their interactions only. When we consider a single electron-hole pair in the crystal, the Hamiltonian reduces to $K_e + K_h + V_{eh}$, where K_e and K_h are the kinetic terms, and V_{eh} is the electron-hole Coulomb interaction. Its eigenstates include bound states, the excitons, with a binding energy E_B, and a Bohr radius a_B. Also a state of the crystal with two excitons approximately diagonalizes the total Hamiltonian, apart from terms of the order of a_B^2/S, S being the sample surface. We may iterate this argument, and understand that when $n_{exc}a_B^2 \ll 1$ (n_{exc} the exciton density), the system may be treated as an ideal bose gas of excitons. We remark that this bosonic concept is very valuable. For example, it is awkward (though possible) to describe an exciton condensate in the electron-hole basis. However, the description of the exciton as an ideal boson is seldom sufficient. Even when $n_{exc}a_B^2 \ll 1$, there is a small but finite overlap of the exciton constituents: as they are fermions, they should not overlap. It is possible to still treat the excitons as bosons, by including an effective repulsion between them such that the overlap of the fermionic constituents is reduced. This procedure can be formalized, under the assumption that excitons only are present: the fundamental microscopic Hamiltonian may be mapped to a bosonic Hamiltonian, featuring the exciton kinetic energy term as the lowest-order term, and higher-order terms representing two-body, three-body, and so on, exciton interactions. Among these systematic methods for constructing the higher-order terms, we recall the commutator expansions,[12] and ordering/transcription operators methods.[13,14] Of course, all give the same results. In practice, we have to truncate the bosonic Hamiltonian to some finite order. The simplest truncation consists of neglecting exciton-exciton interactions altogether, and was discussed above. The two-body exciton interaction is the lowest order term, which takes into account the fermionic nature of the exciton constituents. In this paper we include the two-body interaction only, and neglect higher-order terms. The truncated Hamiltonian is used to cal-

culate dynamical effects to all orders, nonperturbatively.[15] In principle, the remainder of the interaction could introduce contributions comparable to the calculated ones. To the best of our knowledge, even the convergence problem has not been addressed in general. The justification is after all phenomenological, in that truncating up to the two-body interaction, we achieve a satisfactory description of the dynamics of the real system. For thermal equilibrium, it is well known that the two-body interactions are necessary for the description of the second-order phase transitions.[16] In the exciton case we have another phase transition (Mott transition) to the electron-hole plasma when $n_{exc}a_B^2 \sim 1$, which we can clearly not describe in the bosonic model of excitons introduced above. We conclude that the bosonic description of the system, including two-body interaction, is probably sufficient to describe the dynamics when $n_{exc}a_B^2 \ll 1$.

A. Exciton-exciton interaction

The exciton-exciton interaction Hamiltonian reads:

$$H_{exc\text{-}exc} = \sum_{\mathbf{k},\mathbf{k}',\mathbf{q}} M_{\mathbf{k}_1,\mathbf{k}_2,\mathbf{q}}\, b^\dagger_{\mathbf{k}_1+\mathbf{q}} b^\dagger_{\mathbf{k}_2-\mathbf{q}} b_{\mathbf{k}_1} b_{\mathbf{k}_2}, \qquad (1)$$

where we omitted to indicate spin degrees of freedom. The actual calculation of the two-body interaction was already carried out in details in the literature, including the spin degrees of freedom.[17,18,14] We report a straightforward derivation in Appendix A. In the GaAs quantum well, for heavy-hole excitons we have four exciton spin states, of which two are dark. Rapid scattering between the different spin states equalizes their population. In the following we do not address this equalization dynamic, but consider the exciton population at later times, when all spin states are equally populated. Therefore, we average out the spin degrees of freedom in the scattering matrix elements, which results in using 1/2 of the value of $|M|^2$ for aligned spins. Both exchange of consituents and direct Coulomb interaction contribute to this value of $M_{\mathbf{k}_1,\mathbf{k}_2,\mathbf{q}}$. However, direct Coulomb interaction (of dipole-dipole type), is much weaker than the short-ranged exchange, and here we neglect it completely. For small momenta $k,k',q \ll a_B^{-1}$:

$$M \sim 2\sum_{\mathbf{k},\mathbf{k}'} V_{\mathbf{k}-\mathbf{k}'}\phi_{\mathbf{k}}\phi_{\mathbf{k}'}[\phi_{\mathbf{k}}^2 - \phi_{\mathbf{k}}\phi_{\mathbf{k}'}] \sim 6E_B\frac{a_B^2}{S}, \qquad (2)$$

Here $V_{\mathbf{k}} = 2\pi/(Sk)$ is the two-dimensional Coulomb interaction, and $\phi_{\mathbf{k}} = \sqrt{8\pi a_B^2/S}[1+(ka_B)^2]^{-3/2}$ is the $1s$ two-dimensional exciton wave function. The detailed momentum and angular dependence of $M_{\mathbf{k},\mathbf{k}',\mathbf{q}}$ are reported in Appendix A, and have been calculated numerically in Refs. 18 and 19. They typically show a momentum cutoff of the order of a_B^{-1}, which we neglect as we will consider cold distributions spanning a smaller phase space.

B. Higher-order exciton-photon interaction

The bosonization of the interaction Hamiltonian between electron and holes and photons is straightforward, and given in Appendix A. The linear interaction term reads

$$H^{(2)}_{eh\text{-}phot} = \sum_{\mathbf{q}} \frac{\Omega}{2} (b^{\dagger}_{\mathbf{q}} + b_{-\mathbf{q}})(a_{\mathbf{q}} + a^{\dagger}_{-\mathbf{q}}), \qquad (3)$$

where Ω is the Rabi splitting, and is related to the material and electromagnetic field quantization parameters.[20] Higher-order terms are also calculated directly in the fermionic space in Appendix A, and result into

$$H^{(4)}_{eh\text{-}phot}$$

$$= \sum_{\mathbf{k}_1,\mathbf{k}_2,\mathbf{q}} \sigma_{\mathbf{k}_1,\mathbf{k}_2,\mathbf{q}} (b^{\dagger}_{\mathbf{k}_1+\mathbf{k}_2-\mathbf{q}} b_{\mathbf{k}_1} b_{\mathbf{k}_2} + \text{H.c.})(a_{\mathbf{q}} + a^{\dagger}_{-\mathbf{q}}), \qquad (4)$$

with $\sigma_{\mathbf{k}_1,\mathbf{k}_2,\mathbf{q}}$ given in Appendix A. In the limit of $k_1, k_2, q \ll a_B^{-1}$

$$\sigma \sim \frac{4\pi}{7} \frac{a_B^2}{S} \Omega. $$

This nonlinear exciton-photon interaction term is the bosonic counterpart of the phase space filling in the interaction of electrons and holes with photons. In the microcavities that we are considering, $\Omega \sim 4$ meV, while $E_B \sim 10$ meV. In the calculation of the scattering to polaritons, the matrix elements are squared. This nonlinear interaction gives a contribution of order $(\Omega/4E_B)^2 \sim 10^{-2}$ compared to exciton-exciton scattering, and is fairly negligible. Thus, phase-space filling is negligible in the microcavity polariton system. The collapse of Rabi splitting originates in the broadenings from exciton-exciton interaction, when $\hbar\Gamma_{exc-exc} \sim \Omega/2$, as remarked in Ref. 21, rather than in a saturation of the oscillator strength in the optical transition. Instead, for systems having $\Omega > E_B$, such as the bulk GaAs, we should also take this term into account.[22]

III. RATE EQUATION MODEL OF THE DYNAMICS

We may identify three steps in the description of the dynamics of excitations: first excitations are provided either continuously or impulsively by an external pump, second a relaxation process in which the energy is exchanged between the excitations and with the lattice, and finally a radiative recombination process. In the continuous case, the stationary state of the system is produced by the balance between these processes. Emission is measurable only for those states that are radiatively recombining, and is defined as the rate of photon emission into a defined solid angle. In this paper we are considering direct injection of excitons in the system at low temperatures. This allows us to disregard completely the presence of free carriers and exciton formation and ionization processes. The relaxation and recombination steps are characterized by different characteristic time scales. In the following, we are going to keep track of all these different time scales exactly within a semiclassical rate equation model of the dynamics. In the numerical calculations we need to discretize the k space. In a finite volume calculation, the k-space mesh is uniform. However, the excitons and polaritons have largely different masses. A dense grid for the polariton would result in an exciton grid with a prohibitively large number of points. Thus, in this paper we choose instead a grid that is uniformly spaced in energy. We also assume
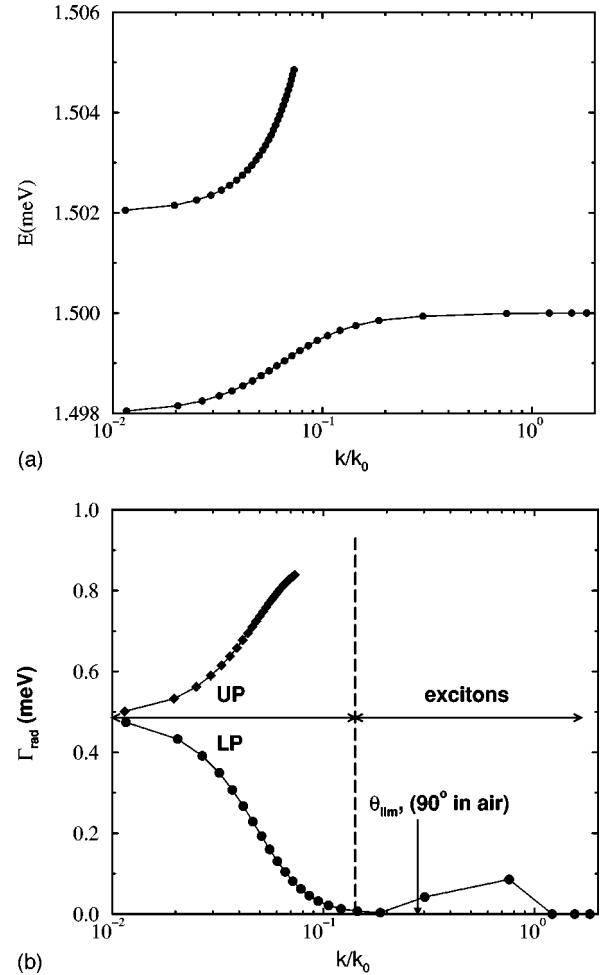

FIG. 1. (a) The exciton-polariton dispersion at small k. (b) The radiative recombination rates. The symbols mark the points used for discretization, evenly spaced in energy. The lines are only guidelines for the eye. The radiative rates of excitons having $k > k_0 = n\omega/c = 0$.

isotropic populations. The uniform energy grid allows us to impose exact energy conservation in the elastic exciton-exciton scatterings, and avoids numerical drifts in the energy conservation from the elastic terms in the integration of the rate equations. This point is important, as our problem contains different time scales, and many hundred integration steps are required to reach stationarity. The grid for the lower polariton branch (which includes excitonlike polaritons) is defined as

$$E_i^{(j)} = E^{(1)}(k=0) + (i+1/2)\Delta E, \qquad (5)$$

with $i = 0, 1, \ldots,\ j = 1, 2$. Here ΔE defines the energy spacing, $j = 1$ labels the lower branch, and $j = 2$ the upper branch. We used the same energy grid for both UP and LP, which makes it immediate to write energy conservation in the elastic scatterings. In the following, we will use one index only to label both the energy bin and the branch for compactness. The energy grid defines a nonuniform k grid, $\{k_i\}$, such that $E(k_i) = E_i$.

The discrete rate equations then read

$$\dot{N}_i = P_i - \Gamma_i N_i - W_{i,i'} N_i(N_{i'}+1) + i \leftrightarrow i'$$

$$- Y_{ii_1,i'i_1'} N_i N_{i_1}(N_{i'}+1)(N_{i_1'}+1) + \begin{matrix} i \leftrightarrow i' \\ i_1 \leftrightarrow i_1' \end{matrix}, \quad (6)$$

and repeated index are summed. Here Γ_i are the radiative recombination rates, $W_{i,i'}$ the exciton (or polariton) scattering rates with the phonons, $Y_{ii_1,i'i_1'}$ the exciton (or polariton)-exciton scattering rates, and N_i is the population at k_i.

A. Dispersion and radiative recombination

The calculation of the exciton-polariton dispersion is straightforward within the two-oscillator model,[23] and the energies thus obtained are sufficiently accurate for the calculation of the exciton-phonon and exciton-exciton scattering rates. The radiative recombination rates at small angles may be also derived from this model. At larger angles and k, the detailed structure of exciton-radiative recombination dynamics is related to the leaky modes of the dielectric mirrors.[4] Although the average radiative rates do not markedly differ

from those of the bare (QW), the detailed structure of the transition region between small and large k vectors still depends on the dielectric structure enclosing the QW. Here we carried the calculation of $\Gamma(k)$ for a GaAs based λ-Ga$_{0.7}$Al$_{0.3}$As microcavity embedding a 80 Å QW at its center, and enclosed by a 16 $\lambda/4$ pairs distributed Bragg reflector at the top (facing air), and 24 bottom pairs facing the substrate, according to Ref. 25. The low index of refraction material in the mirrors is AlAs, the high index of refraction one is Ga$_{0.85}$Al$_{0.15}$As. We then averaged the radiative recombination rates over a discrete energy grid [Eq. (5)] having $\Delta E = 0.05$ meV. The resulting energy dispersion and radiative recombination rate as a function of the exciton (polariton) momentum are shown in Fig. 1.

B. Exciton-phonon and exciton-exciton scattering rates

In this section we report the expression for W and Y of Eq. (6) using the Fermi Golden rule. The calculation of the elastic exciton-exciton scattering rate follows that of Snoke and Wolfe.[26] We take the small momenta limit of the interaction matrix element $M_{\mathbf{k}_1,\mathbf{k}_1,\mathbf{q}}$ as explained in Sec. II A:

$$Y_{i_1 i_2,i_3 i_4} = \frac{\pi}{\hbar} \frac{S^2}{(2\pi)^4} \frac{\Delta E^2}{\partial_{k^2}E(k_2)\partial_{k^2}E(k_3)} X_{k_1} X_{k_2} X_{k_3} X_{k_4} \; |M|^2 \frac{R(k_1,k_2,k_3,k_4)}{\partial_{k^2}E^{(j_4)}(k_4)}, \quad (7)$$

$$R(k_1,k_2,k_3,k_4) = \frac{1}{2}\int_{\mathcal{I}} \frac{dx}{\sqrt{[(k_1+k_3)^2-x][x-(k_1-k_3)^2][(k_2+k_4)^2-x][x-(k_2-k_4)^2]}}, \quad (8)$$

$$\mathcal{I} = [(k_1-k_3)^2,(k_1+k_3)^2] \cap [(k_2-k_4)^2,(k_2+k_4)^2].$$

Here $\partial_{k^2}E(k_i) = \partial E(k)/\partial(k^2)|_{k=k_i}$ is proportional to the inverse DOS of the branch j at $k = k_i$. Conservation of energy is automatically imposed, as $k_4 = k(E_4 = E_1 + E_2 - E_3)$. The X_k are the exciton Hopfield coefficients (squared),[24] and specify the exciton content of the polariton state. In the numerical integration, we used adaptive integration in Eq. (8), after changing variable to smooth the singularity at the integration extrema.

The interaction of electrons and holes with acoustic phonons through rigid deformation of the bands is well known, and described in standard textbooks.[27] The resulting interaction with excitons and polaritons has been worked out in details in Refs. 28 and 4, and we only report the final results for the uniform energy grid:

$$W_{i_1,i_2} = \frac{2\pi}{\hbar} \frac{S}{(2\pi)^2} \frac{\Delta E}{2\partial_{k^2}E(k_2)} X_{k_1} X_{k_2}$$

$$\times \frac{\hbar \Delta k}{2\rho S u} R'(k_1,k_2) N_{ph}(E_2-E_1), \quad (9)$$

$$R'(k_1,k_2) = 2\int_0^{\theta_{max}} d\theta \frac{2\Delta k}{\hbar u q_z} I_\perp^2(q_z)$$

$$\times [a_e I_\|(\beta \Delta k_\| a_B) - a_h I_\|(\alpha \Delta k_\| a_B)]^2, \quad (10)$$

with $q_z(\theta) = \sqrt{\Delta k^2 - \Delta k_\|^2}$, $\Delta k_\|^2(\theta) = k_1^2 + k_2^2 - 2k_1 k_2 \cos\theta$, $\Delta k = |E_2 - E_1|/\hbar u$,

$$\cos\theta_{max} = \begin{cases} 1, & c > 1 \\ c, & c \in [-1,1], \\ -1, & c < -1 \end{cases} \quad c = \frac{k_1^2 + k_2^2 - \Delta k^2}{2k_1 k_2}.$$

The phonon occupation factor N_{ph} is the Bose function $N_B(E)$ for $E > 0$ (absorption) and $N_B(E) + 1$ for $E < 0$ (emission). Finally, I are the adimensional overlap integrals representing the effectiveness of overlap of the phonon and exciton wave functions, in the growth direction ($I_\perp$) and in-plane ($I_\|$):

$$I_\perp(q) = \int dz |f(z)|^2 e^{iqz}, \quad I_\|(x) = [1 + (x/2)^2]^{-3/2} \quad (11)$$

and $f(z)$ are growth direction confinement functions. We used a simple midpoint rule to define the energy integrations in Eq. (9), and adaptive integration for the angular integration in θ after changing of the variable for smoothing the singularity at the extremum θ_{max}.

Higher-order terms in the exciton-phonon interaction are exciton-exciton scattering processes in which a phonon is also emitted or absorbed. The sequential elastic exciton-

exciton scattering followed or preceded by phonon relaxation, as described in the rate equations, is presumably more important.

C. Discretization and validity of the rate equations

Four factors influence the choice of ΔE. (i) We want a good description of the population distributions, thus the relative variation of these distributions over ΔE should be small. For a Boltzmann distribution, this condition becomes $\Delta E < k_B T$. For a degenerate Bose distribution, it is more stringent. (ii) We want a good description of the scattering with phonons: ΔE must be smaller than the typical energy exchanged with the phonons. This energy amounts to almost 1 meV in thin GaAs QW. (iii) We want a good description of the exciton-exciton scattering, thus a sufficiently small ΔE. (iv) As the exciton-exciton scattering becomes singular for small exchanged momenta, we need to set a minimum ΔE which works as a cutoff, as explained later. We first examined the relevance of (ii) and (iii), studying typical scattering rates from a given initial population distribution. In order to separate the effects (ii) and (iii) from those related to (i), we chose it as a Gaussian with large energy width $\sigma \gg \Delta E$, and studied the exciton-phonon scattering rates and exciton-exciton scattering rates as functions of energy, for various ΔE. In particular, we considered ΔE in the range 0.05 -0.2 meV. We found changes in the overall scattering rates well below a few parts in a hundred in all the cases. We further checked all the results in the numerical analysis presented in the next sections by doubling ΔE: no significant changes were found, consistent with the above checks.

Problem (iv) is related to the validity of the rate equations. In this approach, we consider successive scatterings as independent: the excitations are moving freely most of the time, and experiencing short binary collisions once in a while. No phase information is carried over from one collision to another, and we may calculate the scattering rates within the Fermi golden rule (incoming and outgoing excitations asymptotically free). Both for elastic and inelastic scattering, this condition translates into $\hbar^2 k \Delta k / m \gg \Gamma$, where k is the momentum of the considered excitation, Δk its change in the collision, and Γ the collision rate.[29] The semiclassical approach may become unsuitable for particles having small momenta, unless Γ scales quicker than k to zero: intuitively, low-momentum excitations are the carrying phase over large distances, and collision may become dependent on past ones. For excitons, or massive particles, at low temperatures, scattering with phonons exchanges energies of the order of 1 meV, whereas the rates are much smaller, of the order of 5 μeV/K. Only for the smallest momenta k, the condition $k \Delta k / m \gg \hbar \Gamma$ does not hold for phonon scattering. In GaAs, this region is a small fraction of the radiative region, thus it is fairly negligible unless condensation and/or very low temperatures are considered. For exciton-exciton scattering, the scattering rate is diverging for small exchanged momenta. Thus, for these particular collisions we cannot apply the rate equations. However, when we are discretizing energy, these collision are mostly within an energy bin, and are thus not apparent in the dynamics: ΔE sets a minimum cutoff energy that we need to consider in the dynamics. The validity of the rate equations then reads $\Delta E \gg \hbar \Gamma$, where Γ now is a typical scattering rate. As a meaningful estimate of Γ we consider the total scattering rate off $k=0$ from a given distribution, which is mildly dependent on the shape of the distribution when the momentum dependences in M are neglected:

$$\hbar \Gamma_{exc-exc} = \frac{\pi^2}{2} (n_{exc} a_B^2) \frac{E_B^2}{\hbar^2 / m_{exc} a_B^2}. \quad (12)$$

For a typical GaAs QW, $\hbar \Gamma \sim 1$ meV at $n_{exc} = 10^{10}$ cm^{-2}, and the rate equation certainly hold for $n_{exc} \sim 10^9$ cm^{-2} at low temperatures, whereas results at higher densities should be considered with reserve.

D. Integration of the rate equation: Numerical results

In this section we present the results of the integration of the rate equations [Eq. (6)], considering a resonant pump term of the Gaussian type, centered at the exciton energy $E = 0$, for different temperatures and excitation intensities. In particular, the pump term reads

$$P_i = P e^{-E(k_i)^2 / \sigma^2}. \quad (13)$$

In the following, we choose $\sigma = 0.25$ meV, representative of a quasimonochromatic pump beam, still larger than $\Delta E = 0.05$ meV, but smaller than E_B. In Fig. 2(a) we show the resulting exciton and polariton populations vs energy, for four different pump intensities, and at $T = 4$ K. The resulting total density is also shown on the figure, and is basically determined by the averaged exciton radiative recombination rate.[30] At low densities, the excitons at $E > 0$ are quasithermal, populated with a Boltzmann factor (a linear tail in logarithmic scale). Instead, both UP and LP are strongly depleted with respect to this thermal population. This is the bottleneck effect discussed in detail in Ref. 6. We may also notice a residual dip for the radiative excitons close to $E = 0$, due to slow phonon scattering at these low temperatures compared to exciton radiative recombination. This was already studied in Ref. 28. Increasing the density, exciton-exciton scattering becomes relevant. This results in a sizeable filling of the depleted LP and UP populations. Also, the residual dip of the radiative excitons at $E = 0$ fills up, disappearing at densities around 10^9 cm^{-2}. In Fig. 2(b) we show the same calculation for $T = 10$ K. The same pump densities were used to generate these data. We remark that larger densities correspond to the same pump rates at $T = 10$ K, as the average radiative lifetime increases with temperature.[30] We may otherwise observe the same qualitative behavior described above for $T = 4$ K. Depletion of the LP and UP, and especially of radiative excitons, are slightly less marked, because of faster phonon scattering.

Another interesting result is found for $T = 4$ K in the energy interval -0.5 meV $< E < 0$ meV region. These lower polaritons still have dominantly excitonlike character, but a rapidly falling DOS with lowering energy. Moreover, they feature long radiative lifetimes, due to cavity confinement, as clearly shown in Fig. 2(b). This last fact, combined with a sufficiently quick exciton-exciton scattering dynamics at the largest considered densities (despite the reduced DOS), is sufficient to guarantee a quasithermal population of the modes. It results in an occupation factor larger than one for some of them, i.e., a dynamical condensation effect for
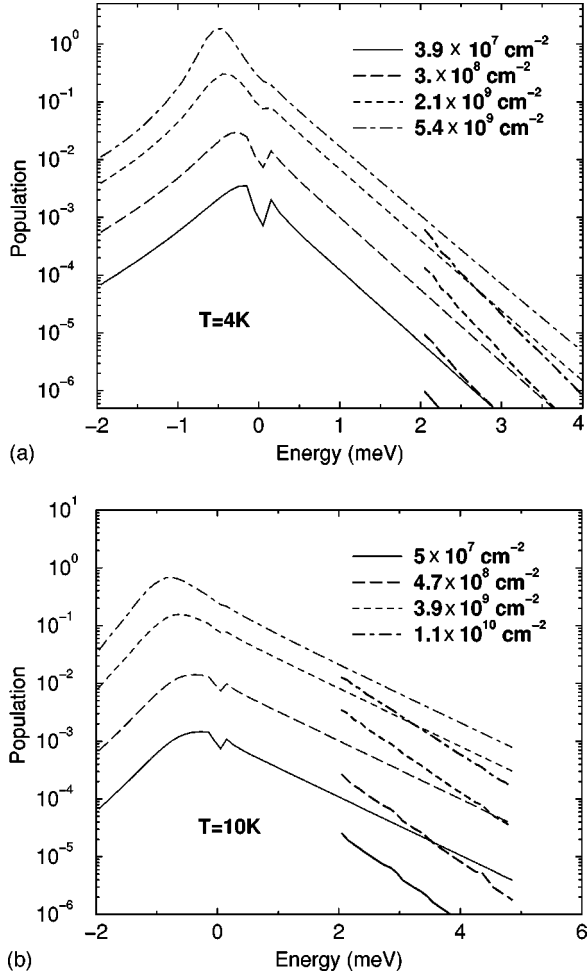
FIG. 2. The exciton and LP population vs energy at different densities, at (a) $T=4$ K, (b) $T=10$ K. The UP population is marked by thicker lines, starting at $E=2$ meV.

$n_{exc}\sim5\times10^{9}$ cm^{-2}. However, we remarked above that in this region of densities results of the rate equations should be considered with reserve, as the exciton-exciton scattering rates are already considerably large. Thus, these results must wait for further analysis beyond the rate equation, which is beyond the scope of the present paper.

IV. STIMULATED SCATTERING

Results of Sec. III confirm the persistence of the bottleneck in the relaxation of excitons to LP up to relatively large densities, which was previously only shown to hold at low densities in Ref. 6. Although spanning a small region of phase space, the scattering dynamics to the polaritons is new with respect to the exciton system. In particular, we enumerate the possible dynamical paths from excitons to LP and UP:

(1) exciton → LP + phonon
(2) exciton → UP± phonon
(3) exciton + exciton → LP + exciton
(4) exciton + exciton → UP + exciton
(5) exciton + exciton→ LP + UP.

The bottleneck in the relaxation of excitons means that the system is strongly out of equilibrium, and an additional LP

population, completely independent of the exciton population, may be injected using a pump at the LP energy. We expect that large LP populations can be thus realized: the scattering to close-by modes is expected to be much smaller than the radiative recombination rate (few ps^{-1}), due to the small LP DOS. In fact, although we noticed in Sec. III C that the scattering out of a single mode is not correctly treated in the rate-equation approach, Eq. (12) still gives a reasonable estimate of this rate when rescaled by $m_{LP}/m_{exc}\sim10^{-4}$. Thus, the scattering rate out of the excited LP mode is always negligible compared to the large LP radiative recombination rates. This is quite the opposite for the excitons, where substantial diffusion to other k states is expected, giving rise to large densities, comparable to the Mott density, well before large populations are realized in the pumped mode. This argument is again based on the different DOS of excitons and LP and is very general. In this discussion we did not include the effects of disorder, which are qualitatively different and will be discussed later in more details. In the above argument we neglected scatterings from LP to excitons or unbound electron-hole pairs, which have relevant final DOS. These processes are suppressed at low temperature, in particular the scattering to excitons for $k_{B}T<\Omega/2$, and optical phonon absorption below 40 K typically in GaAs based structures. In summary, we neglect scattering out of the pumped LP mode at $k=0$ completely, apart from radiative recombination. The possibility of realizing large populations is intimately connected to the bosonic nature of the LP. In particular, processes (1), (3), and (5) are stimulated by large LP populations. The scattering rate related to process (5) may be measured from the UP emission rate. Instead, showing a direct signature of stimulation, observation of the stimulated scattering rates of processes (1) and (3) remains experimentally difficult to access.

In the following we will elucidate the scattering process (1) to (5) in detail. We showed in Sec. III D, that the exciton population is largely of the Boltzmann type. We then assume a rigid exciton distribution of the Boltzmann type $N_{\mathbf{k}}=f_{\mathbf{k}}n_{exc}$, where n_{exc} is the exciton density, and

$$f_{\mathbf{k}}=\mathcal{N}e^{-E(\mathbf{k})/K_{B}T},\ \ E(\mathbf{k})>E_{cut},\qquad(14)$$

$$\mathcal{N}^{-1}=\int\frac{d\mathbf{k}}{(2\pi)^{2}}e^{-E(\mathbf{k})/K_{B}T}$$

is the normalization. In the following, we consider $E_{cut}\sim-0.2$ meV from the numerical results of Sec. III D, in order to take into account populated excitons in the bottleneck region at low density, as shown in Fig. 2. We then reduce the set of rate equations Eq. (6) by discarding irrelevant processes, and fixing rigidly the exciton distribution as above. We also remark that $N_{\mathbf{k}=0}^{(1)}=N_{LP}$ can eventually be large, but otherwise LP and UP populations are negligibly small compared to one:

$$\frac{dN_{UP,\mathbf{k}}}{dt}=-\frac{N_{UP,\mathbf{k}}}{\tau_{UP,\mathbf{k}}}+a_{UP,\mathbf{k}}n_{exc}+[b_{UP,\mathbf{k}}+b_{\mathbf{k}}'(1+N_{LP})]n_{exc}^{2}$$

$$(15)$$

$$\frac{dN_{LP}}{dt} = P_{LP} - \frac{N_{LP}}{\tau_{LP}} + a_{LP,\mathbf{k}=0} \ n_{exc}(1+N_{LP})$$

$$+ \left[b_{LP,\mathbf{k}=0} + \sum_{\mathbf{k}} b'_{\mathbf{k}} \right] n_{exc}^2 (1+N_{LP}), \qquad (16)$$

$$\frac{dN_{exc}}{dt} = P_{exc} - \frac{N_{exc}}{\tau_{exc}}$$

$$- \left[a_{LP,\mathbf{k}=0} n_{exc} + \sum_{\mathbf{k}} b'_{\mathbf{k}} n_{exc}^2 + b_{LP,\mathbf{k}=0} n_{exc}^2 \right] N_{LP}.$$

$$\qquad (17)$$

Here $N_{LP,\mathbf{k}}$ and $N_{UP,\mathbf{k}}$ are the LP and UP population at $\mathbf{k}$ respectively, $N_{exc} = n_{exc}S$ the total exciton population, $\tau_{LP} = (\Gamma_{\mathbf{k}=0}^{(1)})^{-1}$ is the LP lifetime, $\tau_{UP,\mathbf{k}}$ the UP radiative lifetime, and τ_{exc} is the averaged radiative lifetime, given by $\tau_{exc}^{-1} = \Sigma_{\mathbf{k}} \Gamma_{\mathbf{k}} f_{\mathbf{k}}$. In Eq. (17) we also neglected those scatterings involving LP and UP that are not stimulated, as from the results of the previous section we know that they have negligible effects on the exciton density. Also, the out-scattering rates from the LP and UP have been neglected, apart from the radiative recombination.

The coefficients a and b can be calculated as usual with the Fermi golden rule:

$$a_{j,k_2} = \frac{2\pi}{\hbar} \frac{S}{(2\pi)^2} \int \frac{dE_1}{2\partial_{k^2}E(k_1)} X_{k_1}^{(1)} X_{k_2}^{(j)} \frac{\hbar\Delta k}{2\rho Su}$$

$$\times R'(k_1,k_2) N_{ph}(E_2 - E_1) f_{k_1}, \qquad (18)$$

where R', N_{ph}, Δk, and all other quantities have been introduced in relation to Eq. (10), and $j=1,2$ for LP and UP, respectively. This rate can be calculated analytically for $j=2$ (Appendix B).

The quadratic coefficients are given by

$$b_{j,\mathbf{k}_3} = \frac{\pi}{\hbar} \frac{S^2}{(2\pi)^4} \int dk_1^2 dk_2^2 X_{k_1}^{(1)} X_{k_2}^{(1)} X_{k_3}^{(j)} X_{k_4}^{(1)} |M|^2$$

$$\times \frac{R(k_1,k_2,k_3,k_4)}{\partial_{k^2}E^{(1)}(k_4)} f_{\mathbf{k}_1} f_{\mathbf{k}_2}. \qquad (19)$$

Due to the small LP and UP DOS, the major contribution originates from excitons as final scattering states in $\mathbf{k}_4$, while scattering to LP is negligible in comparison. As a consequence, it can be shown that for $\mathbf{k}_3 = 0$, $b_{LP} = b_{UP}$. Also, neglecting the small contribution from the populated excitons below $E=0$, we calculated these rates analytically in Appendix B.

We plot in Figs. 3(a) and 3(b) the linear coefficients a of Eq. (18) and quadratic coefficients b of Eq. (19), respectively, as functions of the lattice temperature T, and for $k_3 = 0$. Other parameters regarding the structure were given before. In Fig. 3(a) we see that the scattering to the UP first increases rapidly with T, then only linearly increases for $k_B T > \Omega/2$. The scattering to LP is weakly dependent on T. In Fig. 3(b) we see that the LP and UP coefficients are basically the same for $k=0$. Their temperature dependence is first exponential with temperature, then for $k_B T > \Omega/2$ starts
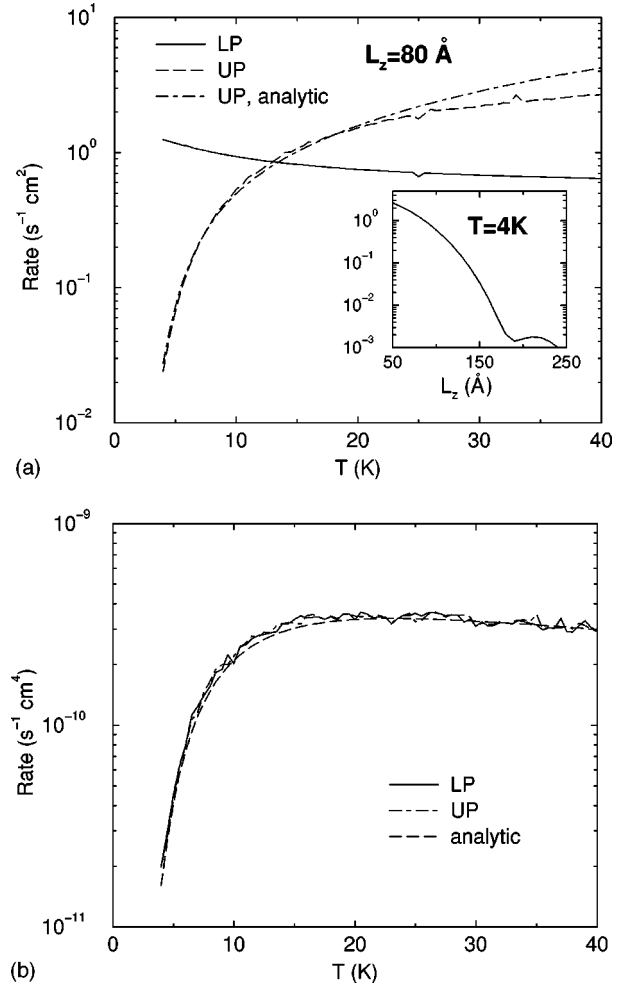

FIG. 3. The scattering coefficients into LP and UP with phonons, a of Eq. (18), in (a), and the exciton-exciton scattering coefficients into LP and UP, b of Eq. (19), in (b), as functions of the lattice temperature T. The analytic approximations of Appendix B are also shown for comparison.

to be weakly decreasing with T. The numerical results compare reasonably well with analytic expressions. As remarked in Appendix B, the phonon scattering to the LP $a_{LP,\mathbf{k}=0}$ is strongly sensitive the the q_z cutoff in the phonon scattering [Eq. (10)]. For QW with infinite barriers, we show its dependence on the QW thickness L_z in the inset of the figure.

The linear and quadratic coefficients show simple exponential dependences on the final energy E, which mainly originate in the Boltzmann factors of the exciton population. Further energy dependences stem from the changes in the exciton components of the final state (Hopfield factors). The energy dependences are found to be well described by the analytic approximation in Appendix B, Eqs. (B1) and (B2) and Eq. (B3). The only exception is the phonon scattering to the LP, which does not show the exponential energy dependence of the other processes. Instead, this rate is more sensitive to the q_z cutoff in the phonon scattering as remarked above.

The coefficient $b'_{UP,\mathbf{k}_3}$ has the same expression as $b_{2,\mathbf{k}_3}$ of Eq. (19), where we now consider the final scattering state $\mathbf{k}_4 = 0$, and $\mathbf{k}_2 = \mathbf{k}_3 - \mathbf{k}_1$:

$$b'_{UP,\mathbf{k}_3} = \frac{\pi}{\hbar} \frac{S}{(2\pi)^2} \int d\mathbf{k}_1 X^{(1)}_{k_1} X^{(1)}_{k_2} X^{(2)}_{k_3} X^{(1)}_{k_4=0} |M|^2 \delta(E_1 + E_2 - E_3 - E_{LP}) f_{\mathbf{k}_1} f_{\mathbf{k}_2}$$

$$= \frac{\pi}{\hbar} \frac{S}{(2\pi)^2} |M|^2 X^{(2)}_{k_3} \frac{1}{2} \int \frac{dE_1}{\partial_{k^2} E_2} \frac{X^{(1)}_{k_1} X^{(1)}_{k_2}}{\sqrt{[(k_2+k_3)^2 - k_1^2][k_1^2 - (k_2+k_3)^2]}} f_{\mathbf{k}_1} f_{\mathbf{k}_2}. \tag{20}$$

This rate is also calculated analytically in Appendix B. We remark that $b' \propto S^{-1}$, as $M^2 \propto S^{-2}$. The stimulated rate is proportional to the $k=0$ LP density $n_{LP} = N_{LP}/S$. We plot the temperature and energy dependence of this rate in Fig. 4. Regarding the energy dependence of the emission at $E = E(k_3)$, it is mostly exponential again. A small reduction in the normal direction $[E = E(k=0)]$ in an energy range of the order of $\hbar^2 k_0^2/2m_{exc}$ (0.1 meV in GaAs) is related to the details of the exciton-polariton dispersion at the knee between the excitons and LP, and is not predicted by the simplified analytic expression in Appendix B. However, in the calculation we neglected the populated dark spin states, which clearly do not split into polariton modes at small momenta, so that it is unlikely to observe this small reduction in actual experiments. We finally checked that all the rates are weakly dependent on the choice of E_{cut}, as expected from the rapidly falling DOS for the exciton modes having $E < 0$.

At small exciton and LP densities, the exciton density n_{exc} is directly proportional to the exciton pump intensity P_{exc}. Thus, the UP emission rate [Eq. (15)] has a linear contribution in P_{exc} originating from process (2), and two quadratic contributions in P_{exc} originating from processes (4) and (5). The latter is also proportional to the LP population in the $k=0$ mode, thus to P_{LP}. Experimentally, it is thus possible to discriminate between the three contributions from their different power-law dependences on P_{exc} and P_{LP}. For example, at $T=4$ K, considering $n_{exc} = 10^9$ cm^{-2}, we obtain $a_{UP,k=0} n_{exc} \sim 2 \times 10^7$ s^{-1}, and also

$b_{UP,k=0} n_{exc}^2 \sim 2 \times 10^7$ s^{-1}, which are quite measurable emission rates. When also $n_{LP} = N_{LP}/S = 10^9$ cm^{-2}, $b'_{k=0} n_{exc}^2 n_{LP} \sim 10^8$ s^{-1}: the stimulated scattering of exciton into polaritons is measurable, and dominates the other scatterings already at small LP densities. All the three scattering processes have been actually observed and discriminated in experiments at 4.8 K.[33] We finally remark that increasing the temperature reduces the stimulated scattering rate in comparison to types (2) and (4) scatterings, making more difficult its observation.

V. SATURATION DYNAMICS

For large n_{LP} and large n_{exc}, the scattering of excitons into LP competes with the exciton radiative recombination: the last three terms of Eq. (17) then become comparable to the radiative recombination term. As a result, the exciton population becomes sublinear in P_{exc}. Already at low temperatures, here we will consider $T=4$ K, the contribution from $\Sigma_k b'_{\mathbf{k}}$ in Eq. (17) is actually smaller by one order of magnitude with respect to that of processes (1) and (3). Thus, we further simplify Eqs. (16) and (17) to analyze the resulting saturation dynamics in stationary conditions:

$$\frac{n_{exc}}{\tau_{exc}} = \frac{P_{exc}}{S} - [a_{LP,k=0} n_{exc} + b_{LP,k=0} n_{exc}^2] n_{LP} \tag{21}$$

$$\frac{n_{LP}}{\tau_{LP}} = \frac{P_{LP}}{S} + [a_{LP,k=0} n_{exc} + b_{LP,k=0} n_{exc}^2] n_{LP}. \tag{22}$$

The UP emission rate is still given by Eq. (15). We plot in Fig. 5 the dependence of this rate as a function of P_{LP},
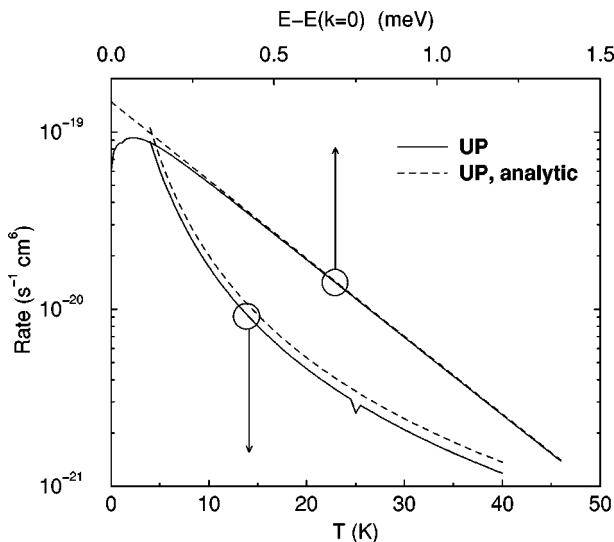

FIG. 4. The scattering rate to both LP and UP, as a function of the UP energy, and as a function of temperature T, for $T=4$ K and for $E - E(k=0) = 0.2$ meV, respectively. The analytic approximations of Appendix B are also shown for comparison.
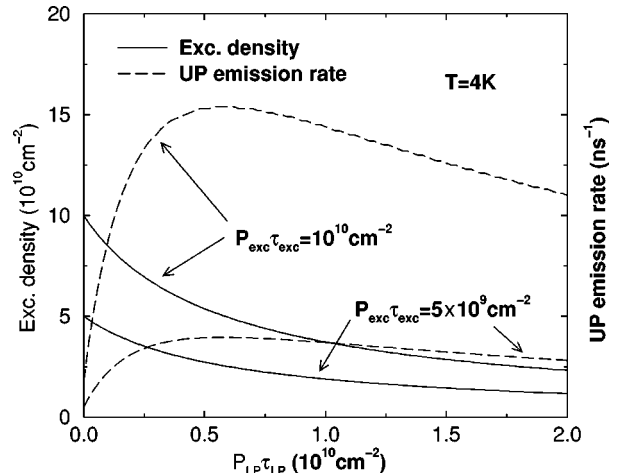

FIG. 5. The scattering rate to the UP, and the total exciton density, as functions of the LP density, for $T=4$ K and two different, fixed exciton pump rates P_{exc}.

considering a fixed pump rate $(P_{exc}/S)\tau_{exc}=10^{10}$ cm^{-2} s^{-1} and a fixed-averaged radiative lifetime for the excitons of 100 ps. These are typical parameters for a GaAs QW. As expected, the UP emission rate first increases linearly with P_{LP}, then saturates and starts to decrease. The saturation is related to the reduction of n_{exc} for increasing n_{LP}. Both the linear (phonon mediated) and quadratic rates consequently finally decrease, resulting in a sublinear dependence on P_{LP}. For even larger P_{LP}, the decrease of n_{exc} is so marked that it results in a net reduction of the UP emission rate. For smaller P_{exc} the saturation of the UP emission rate is less marked.

The results shown in Fig. 5 have to be considered as qualitative only, as $n_{exc}>10^9$ cm^{-2}: we have already remarked in Sec. III C that the rate equation approach becomes unsuitable when the exciton-exciton scattering rates are larger than typical energies, here $k_B T < \Omega$. We may expect that multiple scattering has to be effectively included in this case. A self-consistent Born approximation, leading to generalized rate equations, could still be insufficient when the excitons become almost degenerate.[29] Furthermore, even when $n_{exc} < 10^9$ cm^{-2}, a large n_{LP} induces a relevant exciton-mass renormalization, and further reduction of the scattering rates as their dispersion becomes phononlike, in analogy to superfluidity. Preliminary calculations show that this effect is already relevant well below $n_{LP} \sim 10^{10}$ cm^{-2}.[31] We may instead neglect LP mass renormalization effects due to the usual small DOS. Finally, the collapse of the Rabi splitting, which can be thought of as a polariton-energy renormalization, sets in abruptly at $n_{exc} \sim 4 \times 10^{10}$ cm^{-2}:[32] it is therefore relevant in a narrow region of densities close to the above one, and below this critical density, the effects of the LP and UP energy renormalization remain negligible, and we did not consider them in this paper.

VI. DISCUSSION AND CONCLUSIONS

We have confirmed the persistence of the bottleneck effect up to large exciton densities, and shown how to exploit the resulting nonequilibrium to perform experiments that evidentiate the bosonic character of LP and UP. In particular, the scattering of two excitons into both LP and UP can be enhanced by final-state stimulation using an external beam that injects a large LP population. The resulting UP emission rate is linearly dependent on the LP beam intensity at low densities, and the calculated rates show that this process is measurable at modest exciton and LP densities. Preliminary experimental results confirm this expectation.[33] Moreover, we investigated the saturation effects of the UP emission, within the rate equations approach, and showed that they are observable for exciton and LP densities around $n_{LP} \sim 10^{10}$ cm^{-2}, well below the collapse of the Rabi splitting. We discussed other important renormalization effects that are not included in the rate equations. These are expected to further enhance the saturation effects. Finally, we recalled how the present bosonization approach partially includes the fermionic properties of the microscopic elementary excitations. Both stimulated exciton-exciton scattering and saturation effects have this same microscopic origin, and the same results are thus expected in the fermionic picture, although their description would be far less transparent.

Stimulated emission of bulk polaritons was already experimentally observed in II-VI samples of sufficient quality in the late seventies,[34] and more recently in QW microcavity samples.[35] In the bulk, a cleaved bulk crystal formed a natural resonator for the photonlike polaritons of the lower branch, increasing their lifetime to several ps. Sufficient excitation produced stimulated emission based on various mechanisms, depending on temperature: from LO phonon emission at high temperature, to exciton-exciton scattering at the lowest temperatures. The gain mechanisms were theoretically characterized by Haug and Koch,[36] based on the same semiclassical approximation of the dynamics we considered in this paper. Large exciton binding energy, strong oscillator strengths (large polariton splittings), and strong exciton-LO phonon interaction, favor the realization of stimulated emission before the polariton splitting collapses at large excitation densities. However, this fact was not checked in any experiment; as in the bulk, the splitting does not directly show in emission or reflectivity, and much more involved experimental techniques are necessary for its observation.[37] The laser emission in the II-VI microcavities occured at large negative detunings only, and persistence of the splitting was not reported either.[35] We remark that in principle, the stimulated *scattering* effects presented in this paper could have been observed even in the bulk, but to the best of our knowledge, the problem was never addressed.

The issue of interface disorder and inhomogeneous broadening in the QW is relevant in currently grown structures. It is presumably leading to important consequences in the polariton dynamics, which have not been addressed in this paper. Excitons are ''motionally narrowed'' in the QW, in the sense that they show only a small fraction, typically few meV, of the full interface potential variation, fractions of an eV, in the optical response. Due to the small DOS, polaritons were predicted to be even more so in a pioneering paper by Whittaker *et al.*[38] However, it has been later shown that for current structures, polaritons and excitons are substantially mixed by multiple scattering with the strong disorder potentials, and have to be treated on an equal footing.[39,40] This resulted in the explanation of a much weaker motional narrowing for the LP, and of its absence for the UP. These latter approaches treat both exciton-photon coupling, and exciton scattering on disorder exactly. Interestingly, a simplified approach, which accounts for effects of disorder at the level of exciton absorption only, was also shown to produce the correct results for the polariton inhomogeneous line widths.[41] This makes questionable the advantage to use the polariton picture when considering strong disorder. Regarding the scattering dynamics with phonons and other excitons, the above results also point out to the insufficiency of the clean polariton picture used in this paper. Indeed, some predictions of the polariton dynamics are in striking contrast to the experimental observations: the detailed photoluminescence lineshape from the LP and UP is predicted to be strongly nonthermal in our model,[6] but is instead found to be at most weakly deviating from thermal emission in experiment.[42] Moreover, recent studies put into evidence shortcomings of the calculation of the photon emission within the simple rate-equation approach, at least for large negative detunings.[43] Finally, no direct observation of the bottleneck dynamics in the microcavity polariton system has yet been reported. In

many respects, the situation has analogies to the early one for the bulk, when the weak lower branch luminescence was completely dominated by emission from impurity-bound excitons, preventing the observation of the exciton-polariton dynamics. Cleaner samples finally allowed for its direct observation. We may expect the same will occur for the microcavities. However, we notice that indirect, but solid, experimental evidence of the bottleneck has already been established: the exciton dynamics of bare and cavity embedded QW is similar, and independent of the exciton cavity detuning,[44] and the LP do not dynamically condense at low-lattice temperatures, before collapse of the Rabi splitting.[9,10] Moreover, evidence of a thermal exciton reservoir is found in the temperature dependence of the exciton lifetime,[30,44] and the possibility to realize large LP population with a pump remains true as the LP lineshape is mainly related to the radiative recombination, and scattering out of LP by phonon absorption has been shown to be quenched at low temperatures.[45] We therefore expect that our predictions of stimulated scattering remain valid also for the current samples, as they are based on the above evidence extracted from current samples. We conclude that although disorder is likely to quantitatively affect the calculated photon-emission rates, the qualitative features of the dynamical picture presented in this paper are relevant also for current samples.

ACKNOWLEDGMENTS

APPENDIX A

Let us consider the fermionic Hilbert space $\mathcal{F}$ of electron-hole pairs, and the bosonic Hilbert space of excitons $\mathcal{B}$. They can be further subdivided in subspaces of 0, 1, 2, ..., n pairs, $\mathcal{F} = \mathcal{F}_0 \oplus \mathcal{F}_1 \oplus \mathcal{F}_2 \oplus \ldots$, and subspaces of 0, 1, 2, ..., n excitons, $\mathcal{B} = \mathcal{B}_0 \oplus \mathcal{B}_1 \oplus \mathcal{B}_2 \oplus \ldots$. The states of the $n = 0$, 1 subspaces may be put into a one-to-one correspondence trivially:

$$c_{p_1}^\dagger d_{q_1}^\dagger |0\rangle_F \leftrightarrow b_{p_1 q_1}^\dagger |0\rangle_B,$$

where $c^\dagger$ and $d^\dagger$ are electron and hole creation operators, and the $b^\dagger$ operators are bosonic creation operators. The dimensionality of $\mathcal{B}_n$ for $n \geq 2$ is much larger than the dimensionality of $\mathcal{F}_n$. For example: $c_{p_1}^\dagger d_{q_1}^\dagger c_{p_2}^\dagger d_{q_2}^\dagger |0\rangle_F$ exists only for $p_1 \neq p_2$, whereas $b_{p_1 q_1}^\dagger b_{p_1 q_1}^\dagger |0\rangle_B$ also exists for $p_1 = p_2$. Thus, the $\mathcal{B}_n$, $n \geq 2$ have to be restricted to "physical" states with some projection operation. In practice, as we are looking for the transcription of bound exciton states only, and to almost empty bands (continuum limit), this restriction is completely avoided. Many approaches have been devised to realize the transcription of bound bosons.[12–14,17] For $n = 2$, it is straightforward to build the corresponding states in the bosonic and fermionic space directly.[17,18] Here, we briefly outline the conceptual steps in the derivation.

We are interested in transcribing the $1s$ bound excitons from $\mathcal{B}_2$ to $\mathcal{F}_2$. First, the correspondence between $\mathcal{B}_1$ and $\mathcal{F}_1$ is trivial:

$$|\mathbf{K}\rangle_B = b_\mathbf{K}^\dagger |0\rangle_B \leftrightarrow |\mathbf{K}\rangle_F = \sum_\mathbf{k} \phi_{\beta\mathbf{K}+\mathbf{k}}^* c_{-\mathbf{k}}^\dagger d_{\mathbf{K}+\mathbf{k}}^\dagger |0\rangle_F . \tag{A1}$$

Here, $\beta = m_h/(m_e + m_h)$. Tentatively, we may try the same correspondence in $n = 2$:

$$|\mathbf{K}_1 \mathbf{K}_2\rangle_B = b_{\mathbf{K}_1}^\dagger b_{\mathbf{K}_2}^\dagger |0\rangle_B \leftrightarrow |\mathbf{K}_1 \mathbf{K}_2\rangle_F$$

$$= \sum_{\mathbf{k}_1, \mathbf{k}_2} \phi_{\beta\mathbf{K}_1+\mathbf{k}_1}^* \phi_{\beta\mathbf{K}_2+\mathbf{k}_2}^* c_{-\mathbf{k}_1}^\dagger d_{\mathbf{K}_1+\mathbf{k}_1}^\dagger c_{-\mathbf{k}_2}^\dagger d_{\mathbf{K}_2+\mathbf{k}_2}^\dagger$$

$$\times |0\rangle_F . \tag{A2}$$

However, the fermionic states are not properly normalized, as $_F\langle \mathbf{K}_1' \mathbf{K}_2' | \mathbf{K}_1 \mathbf{K}_2 \rangle_F = \delta_{\mathbf{K}_1, \mathbf{K}_1'} \delta_{\mathbf{K}_2, \mathbf{K}_2'} \delta_{\mathbf{K}_1, \mathbf{K}_2'} \delta_{\mathbf{K}_2, \mathbf{K}_1'} + O(a_B^2/S)$. Thus, in calculating $_B\langle_B \mathbf{K}_1' \mathbf{K}_2' | \mathcal{O}_B | \mathbf{K}_1 \mathbf{K}_2 \rangle_B$ as $_F\langle \mathbf{K}_1' \mathbf{K}_2' | \mathcal{O}_F | \mathbf{K}_1 \mathbf{K}_2 \rangle_F$, this fact must be taken into account properly. In particular, we are interested in $\mathcal{O}_F = K_e + K_h + V_{ee} + V_{hh} + V_{eh}$. We have,

$$K_e |\mathbf{K}_1 \mathbf{K}_2\rangle_F = \sum_{\mathbf{k}_1, \mathbf{k}_2} [\epsilon_{c\mathbf{k}_1} + \epsilon_{c\mathbf{k}_2}] \phi_{\beta\mathbf{K}_1+\mathbf{k}_1}^* \phi_{\beta\mathbf{K}_2+\mathbf{k}_2}^* c_{-\mathbf{k}_1}^\dagger d_{\mathbf{K}_1+\mathbf{k}_1}^\dagger c_{-\mathbf{k}_2}^\dagger d_{\mathbf{K}_2+\mathbf{k}_2}^\dagger |0\rangle_F . \tag{A3}$$

$$V_{eh} |\mathbf{K}_1 \mathbf{K}_2\rangle_F = \sum_{\mathbf{k}_1, \mathbf{k}_2, \mathbf{q}} V_\mathbf{q} \{ (\phi_{\beta\mathbf{K}_1+\mathbf{k}_1+\mathbf{q}}^* \phi_{\beta\mathbf{K}_2+\mathbf{k}_2}^* + \phi_{\beta\mathbf{K}_1+\mathbf{k}_1}^* \phi_{\beta\mathbf{K}_2+\mathbf{k}_2+\mathbf{q}}^*) c_{-\mathbf{k}_1}^\dagger d_{\mathbf{K}_1+\mathbf{k}_1}^\dagger c_{-\mathbf{k}_2}^\dagger d_{\mathbf{K}_2+\mathbf{k}_2}^\dagger$$

$$+ \phi_{\beta\mathbf{K}_1+\mathbf{k}_1}^* \phi_{\beta\mathbf{K}_2+\mathbf{k}_2}^* c_{-\mathbf{k}_1+\mathbf{q}}^\dagger d_{\mathbf{K}_1+\mathbf{k}_1}^\dagger c_{-\mathbf{k}_2}^\dagger d_{\mathbf{K}_2+\mathbf{k}_2-\mathbf{q}}^\dagger + \phi_{\beta\mathbf{K}_1+\mathbf{k}_1}^* \phi_{\beta\mathbf{K}_2+\mathbf{k}_2}^* c_{-\mathbf{k}_1}^\dagger d_{\mathbf{K}_1+\mathbf{k}_1-\mathbf{q}}^\dagger c_{-\mathbf{k}_2+\mathbf{q}}^\dagger d_{\mathbf{K}_2+\mathbf{k}_2}^\dagger \} |0\rangle_F .$$

The first two terms represent electron-hole Coulomb interaction within the same exciton; together with the terms from $(K_e + K_h) |\mathbf{K}_1 \mathbf{K}_2\rangle_F$, they thus give $(\epsilon_{\mathbf{K}_1} + \epsilon_{\mathbf{K}_2}) |\mathbf{K}_1 \mathbf{K}_2\rangle_F$, where $\epsilon_\mathbf{K}$ is the exciton energy. These terms contribute to the self-energy of the two excitons only, and have to be discarded in the calculation of the scattering-matrix elements. Finally, the calculation of

$$V_{ee} |\mathbf{K}_1 \mathbf{K}_2\rangle_F = \sum_{\mathbf{k}_1, \mathbf{k}_2, \mathbf{q}} V_\mathbf{q} \phi_{\beta\mathbf{K}_1+\mathbf{k}_1}^* \phi_{\beta\mathbf{K}_2+\mathbf{k}_2}^* c_{-\mathbf{k}_1-\mathbf{q}}^\dagger d_{\mathbf{K}_1+\mathbf{k}_1}^\dagger c_{-\mathbf{k}_2+\mathbf{q}}^\dagger d_{\mathbf{K}_2+\mathbf{k}_2}^\dagger |0\rangle_F$$

is straightforward, and the $V_{hh}|\mathbf{K}_1\mathbf{K}_2\rangle_F$ term is analogous. Simple algebra leads to the scattering-matrix elements, which do not have to be further renormalized as they are already of order a_B^2/S:

$$
_F\langle\mathbf{K}_1+\mathbf{Q}\mathbf{K}_2-\mathbf{Q}|V_{ee}|\mathbf{K}_1\mathbf{K}_2\rangle_F=\left\{\sum_{\mathbf{k}_1\mathbf{k}_2}[V_Q-V_{\mathbf{k}_1-\mathbf{k}_2-\mathbf{Q}}]\phi_{\beta\mathbf{K}_1+\mathbf{k}_1-\alpha\mathbf{Q}}\phi_{\beta\mathbf{K}_2+\mathbf{k}_2+\alpha\mathbf{Q}}\phi^*_{\beta\mathbf{K}_1+\mathbf{k}_1}\phi^*_{\beta\mathbf{K}_2+\mathbf{k}_2}\right\}+\{\mathbf{Q}\leftrightarrow\mathbf{K}_2-\mathbf{K}_1-\mathbf{Q}\}.
$$

Here $\alpha=1-\beta$, and $_F\langle\mathbf{K}_1+\mathbf{Q}\mathbf{K}_2-\mathbf{Q}|V_{hh}|\mathbf{K}_1\mathbf{K}_2\rangle_F$ has simply $\alpha\leftrightarrow\beta$. The first term is the classical Coulomb interaction, the second term is the exchange of the electron, the other two are the corresponding exciton (boson) exchanges. Finally, from the last two terms of $V_{eh}|\mathbf{K}_1\mathbf{K}_2\rangle_F$ we obtain:

$$
\begin{aligned}
_F\langle\mathbf{K}_1+\mathbf{Q}\mathbf{K}_2-\mathbf{Q}|V_{eh}|\mathbf{K}_1\mathbf{K}_2\rangle_F=&\left\{\sum_{\mathbf{k}_1\mathbf{k}_2}V_Q[\phi_{\beta\mathbf{K}_1+\mathbf{k}_1+\beta\mathbf{Q}}\phi_{\beta\mathbf{K}_2+\mathbf{k}_2+\alpha\mathbf{Q}}+\phi_{\beta\mathbf{K}_1+\mathbf{k}_1-\alpha\mathbf{Q}}\phi_{\beta\mathbf{K}_2+\mathbf{k}_2-\beta\mathbf{Q}}]\phi^*_{\beta\mathbf{K}_1+\mathbf{k}_1}\phi^*_{\beta\mathbf{K}_2+\mathbf{k}_2}\right.\\
&\left.+V_{\mathbf{k}_1-\mathbf{k}_2-\mathbf{Q}}[\phi_{\beta\mathbf{K}_1+\mathbf{k}_1-\alpha\mathbf{Q}}\phi_{\beta\mathbf{K}_2+\mathbf{k}_2-\beta\mathbf{Q}}+\phi_{\beta\mathbf{K}_1+\mathbf{k}_2-\alpha\mathbf{Q}}\phi_{\beta\mathbf{K}_2+\mathbf{k}_1-\beta\mathbf{Q}}]\phi^*_{\beta\mathbf{K}_1+\mathbf{k}_1}\phi^*_{\beta\mathbf{K}_2+\mathbf{k}_1-\mathbf{Q}}\right\}\\
&+\{\mathbf{Q}\leftrightarrow\mathbf{K}_2-\mathbf{K}_1-\mathbf{Q}\}.
\end{aligned}
$$

Again, the first two terms are direct Coulomb interactions, and the other exchanges of a single constituent. The last terms are the boson exchanges. The detailed momentum dependence for various α has been calculated numerically in Refs. 18 and 19. The spin dependence of the direct and exchange matrix elements is also readily calculated. Detailed angular dependences for all the four scattering channels in any elliptical basis have been reported in Ref. 19. Here we remark that in the limit of $K_1,K_2,Q\ll a_B^{-1}$, the direct terms are negligible, while the exchange terms give

$$
\begin{aligned}
&\langle\mathbf{K}_1+\mathbf{Q}\mathbf{K}_2-\mathbf{Q}|V_{ee}+V_{hh}|\mathbf{K}_1\mathbf{K}_2\rangle\\
&\sim-4\sum_{\mathbf{k}_1\mathbf{k}_2}V_{\mathbf{k}_1-\mathbf{k}_2}|\phi_{\mathbf{k}_1}|^2|\phi_{\mathbf{k}_2}|^2
\end{aligned}
$$

and

$$
\langle\mathbf{K}_1+\mathbf{Q}\mathbf{K}_2-\mathbf{Q}|V_{eh}|\mathbf{K}_1\mathbf{K}_2\rangle\sim4\sum_{\mathbf{k}_1\mathbf{k}_2}V_{\mathbf{k}_1-\mathbf{k}_2}|\phi_{\mathbf{k}_1}|^2\phi_{\mathbf{k}_2}\phi^*_{\mathbf{k}_1},
$$

and result into Eq. (2).

The interaction of electron and holes with photons in a closed microcavity reads:

$$
\begin{aligned}
H_{eh\text{-}phot}=&\sum_{\mathbf{k},\mathbf{q}}\frac{ep_{cv}}{mc}\sqrt{\frac{4\pi\hbar c^2}{\omega_{cav}L_{eff}S}}\\
&\times(c^\dagger_{\mathbf{k}+\mathbf{q}}d^\dagger_{\mathbf{k}}+d_{\mathbf{k}}c_{\mathbf{k}-\mathbf{q}})(a_{\mathbf{q}}+a^\dagger_{-\mathbf{q}}). \quad (A4)
\end{aligned}
$$

Here m is the free-electron mass, p_{cv} the momentum matrix element between valence and conduction band, and L_{eff} is an effective cavity length, which takes into account the fact that dielectric mirrors have a finite (and large) penetration depth.[23] When considering the bosonic term of lowest-order generated from this Hamiltonian, we find a relationship between the Rabi splitting Ω and the constants above:

$$
\frac{\Omega}{2}=\frac{ep_{cv}}{mc}\sqrt{\frac{4\pi\hbar c^2}{\omega_{cav}L_{eff}S}}\sum_{\mathbf{k}}\phi_{\mathbf{k}}.
$$

Higher-order terms are calculated directly in the fermionic space, as before, and result into Eq. (4). The matrix element reads

$$
\begin{aligned}
\sigma_{\mathbf{K}_1,\mathbf{K}_2,\mathbf{Q}}=&\frac{ep_{cv}}{mc}\sqrt{\frac{4\pi\hbar c^2}{\omega_{cav}L_{eff}S}}\\
&\times\sum_{\mathbf{k}}\phi_{\alpha\mathbf{K}_3+\mathbf{k}+\mathbf{Q}-\mathbf{K}_1}\phi^*_{\alpha\mathbf{K}_2+\mathbf{k}}\phi_{\alpha\mathbf{K}_1+\mathbf{k}+\mathbf{Q}-\mathbf{K}_1},
\end{aligned}
$$

$$(A5)$$

with $\mathbf{K}_3=\mathbf{K}_1+\mathbf{K}_2-\mathbf{Q}$. The limit of low momenta has been reported in Eq. (4).

APPENDIX B

In this appendix we calculate analytical approximations of the exciton to polariton scatterings, under the assumption of thermal-exciton population given in Eq. (14), and with $E_{cut}=0$. First, we consider phonon scattering to the upper branch. There are two major contributions, the first important at large temperatures, with $u\Delta k=\Delta E\sim0$ ($\hbar=1$), when $N_{ph}(\Delta E)\sim\Delta E/k_BT$, and originating in a region of width k_BT. In this case, $\Delta k_\parallel\sim k_{exc}=\sqrt{m_{exc}\Omega}$, and $u\Delta k_\parallel\sim0.1$ meV. Thus, for $k_BT>1$ K, we have $q_z\sim\Delta k$, and the cutoffs $I_\parallel,I_\perp\sim1$. The energy integration of Eq. (18) is in a small interval $[E_2-k_BT/4,E_2+k_BT/4]$ and results into

$$
a_{UP,k_2}=\frac{\pi}{u}X^{(2)}_{\mathbf{k}_2}\frac{(a_e-a_h)^2}{\rho u^2}k_BTe^{-\frac{E_2}{k_BT}}. \quad (B1)
$$

The other contribution is for small temperatures, and originates in phonon *absorption*, when $E_1\ll E_2$, and $N_{ph}(\Delta E)\sim\exp[-(E_2-E_1)/k_BT]$. In this case, the q_z is cutoff at $q_z\sim2\pi/L_z$, and the integration in E_1 of Eq. (18) is in the interval $[E_2-2\pi/L_z,E_2]$. Thus,l

$$
a_{UP,k_2}=\frac{2\pi}{u}X^{(2)}_{\mathbf{k}_2}\frac{(a_e-a_h)^2}{\rho u^2}\frac{(2u\pi/L_z)^2}{2k_BT}e^{-(E_2/k_BT)}.
$$

$$(B2)$$

The crossover between the two behaviors is at $k_B T \sim u 2\pi/L_z$. For the LP, the largest contribution is for phonons of large q_z, and $E_1 \sim 0$. Thus, the rate becomes quantitatively more sensitive on the actual form of the cutoff $I_\perp(q_z)$ at large q_z. It can be shown that the rate is then weakly dependent on temperature for $k_B T < \Omega/2$.

We now consider exciton-exciton scattering to the exciton and UP or LP [Eq. (19)]. $R(k_1, \ldots, k_4)$, whose expression is given in Eq. (8), is readily calculated when $k_3 \ll k_1$, giving

$$R(k_1, \ldots, k_4) = \frac{\pi}{2\sqrt{[(k_2+k_4)^2 - k_1^2][k_1^2 - (k_2-k_4)^2]}}.$$

Then, considering that k_4 is on the exciton branch, $k_4^2 \sim k_1^2 + k_2^2 - 2m_{exc}E_3$, and $[(k_2+k_4)^2 - k_1^2][k_1^2 - (k_2-k_4)^2] = 4k_1^2 k_2^2 - 2m_{exc}E_3$. Also, $\partial_{k^2}E(k_4) \sim 1/2m_{exc}$. Substituting in Eq. (19), we obtain

$$b_{j,\mathbf{k}_3} \sim \pi X_{k_3}^{(j)} |M|^2 2m_{exc} \frac{S^2}{(2\pi)^4} \int_{k_1^2 k_2^2 > m_{exc}E_3} dk_1^2 dk_2^2 \frac{\pi}{2\sqrt{4k_1^2 k_2^2 - 2m_{exc}E_3}} f_{k_1} f_{k_2}$$

$$= \pi X_{k_3}^{(j)} |M|^2 m_{exc} \pi \frac{S^2}{(2\pi)^4} \lambda_{th}^4 2\pi m_{exc} k_B T e^{-|E_3|/k_B T}. \tag{B3}$$

Here $E_3 = E^{(j)}(k_3)$ as usual, and $\lambda_{th}^2 = 2\pi/(m_{exc}k_B T)$ is the exciton-thermal wavelength. Also notice the absolute value in the exponential, which makes the LP scattering rate exponentially increasing with smaller $|E_3|$. This has been confirmed by actual numerical integration.

Finally, for the scattering to both LP and UP, we have from Eq. (20), neglecting details of the lower branch dispersion at the knee, and simply considering a pure excitonic dispersion for k_1, k_2, that the integral is trivial and gives $\pi/2$, thus

$$b'_{UP,\mathbf{k}_3} = \pi^2 X_{k_3}^{(2)} \frac{1}{2} \frac{S}{(2\pi)^2} m_{exc} |M|^2 \lambda_{th}^4 e^{-(E_3 + E^{(1)}(\mathbf{k}=0))/k_B T}. \tag{B4}$$

[1] C. Weisbuch, M. Nishioka, A. Ishikawa, and Y. Arakawa, Phys. Rev. Lett. **69**, 3314 (1992).

[2] R. Houdré et al., Phys. Rev. Lett. **73**, 2043 (1994).

[3] For a review, see V. Savona, C. Piermarocchi, A. Quattropani, P. Schwendimann, and F. Tassone, *New Aspects in Optical Properties of Nanostructures* (Gordon and Breach, New York, 1997).

[4] F. Tassone, C. Piermarocchi, V. Savona, A. Quattropani, and P. Schwendimann, Phys. Rev. B **53**, R7642 (1996).

[5] S. Pau, G. Bjork, J. Jacobson, H. Cao, and Y. Yamamoto, Phys. Rev. B **51**, 7090 (1995).

[6] F. Tassone, C. Piermarocchi, V. Savona, A. Quattropani, and P. Schwendimann, Phys. Rev. B **56**, 7554 (1997).

[7] Y. Toyozawa, Prog. Theor. Phys. **12**, 111 (1959).

[8] H. Sumi, J. Phys. Soc. Jpn. **21**, 1936 (1975); W. J. Rappel, L. F. Feiner, and M. F. H. Schuurmans, Phys. Rev. B **38**, 7874 (1988); C. Weisbuch and R. Ulbrich, J. Lumin. **18/19**, 27 (1979); D. E. Cooper and P. R. Newman, Phys. Rev. B **39**, 7431 (1989); F. Askari and P. Y. Yu, *ibid.* **31**, 6643 (1985); P. Wiesner and U. Hein, *ibid.* **11**, 3071 (1975); G. W. 't Hooft, W. A. J. A. van der Pöel, L. W. Molenkamp, and C. T. Foxon, *ibid.* **35**, 8281 (1987); H. Yokoyama, K. Nishi, T. Anan, H. Yamada, S. D. Bronson, and E. P. Ippen, Appl. Phys. Lett. **57**, 2814 (1990).

[9] H. Cao et al., Phys. Rev. A **55**, 4632 (1997).

[10] M. Kira et al., Phys. Rev. Lett. **79**, 5170 (1997).

[11] This applies to systems having a Rabi splitting smaller than the exciton binding energy.

[12] G. Wentzel, Phys. Rev. **108**, 1593 (1957).

[13] T. Usui, Prog. Theor. Phys. **23**, 787 (1960).

[14] E. Hanamura, J. Phys. Soc. Jpn. **29**, 50 (1970).

[15] For a review see E. Hanamura and H. Haug, Phys. Rep., Phys. Lett. **33**, 209 (1977).

[16] S. K. Ma, *Modern Theory of Critical Phenomena* (W. A. Benjamin, Reading, MA, 1976).

[17] F. Čulik, Czech. J. Phys., Sect. A **16**, 194 (1966).

[18] A. I. Bobryesheva, M. F. Miglei, and M. I. Shmiglyuk, Phys. Status Solidi B **53**, 71 (1972); A. I. Bobryesheva, V. T. Zyukov, and S. I. Beryl, *ibid.* **101**, 69 (1980).

[19] C. Ciuti, V. Savona, C. Piermarocchi, A. Quattropani, and P. Schwendimann, Phys. Rev. B **58**, 7926 (1998).

[20] Intraband currents, related to the displacement of these charges by transverse electromagnetic fields, are usually negligible for photon energy comparable to the band gap.

[21] F. Jahnke et al., Phys. Rev. Lett. **77**, 5257 (1996).

[22] In this case it is also insufficient to consider $1s$ excitons only in constructing the polaritons.

[23] V. Savona, L. C. Andreani, A. Quattropani, and P. Schwendimann, Solid State Commun. **93**, 733 (1995).

[24] J. J. Hopfield, Phys. Rev. **112**, 1555 (1958).

[25] V. Savona, F. Tassone, C. Piermarocchi, A. Quattropani, and P. Schwendimann, Phys. Rev. B **53**, 13 051 (1996).

[26] D. W. Snoke and J. P. Wolfe, Phys. Rev. B **39**, 4030 (1989).

[27] H. Stolz, *Time-Resolved Light-Scattering from Excitons*, Springer Tracts in Modern Physics Vol. 130 (Springer-Verlag, Berlin, 1994).

[28] C. Piermarocchi, F. Tassone, V. Savona, A. Quattropani, and P. Schwendimann, Phys. Rev. B **53**, 15 834 (1996).

[29] P. Danielewicz, Ann. Phys. **152**, 239 (1984).

[30] L. C. Andreani, F. Tassone, and F. Bassani, Solid State Commun. **77**, 641 (1991).

[31] G. Klimovitch (private communication).

[32] R. Houdre *et al.*, Phys. Rev. B **52**, 7810 (1995).

[33] F. Tassone, R. Huang, and Y. Yamamoto, cond-mat/9808157 (unpublished).

[34] C. Klingshirn and H. Haug, Phys. Rep. **70**, 315 (1981).

[35] P. V. Kelkar, V. G. Kozlov, A. V. Nurmikko, C. C. Chu, J. Han, and R. L. Gunshor, Phys. Rev. B **56**, 7564 (1997).

[36] H. Haug and S. Koch, Phys. Status Solidi B **82**, 531 (1977).

[37] B. Hönerlage, R. Levy, J. B. Grun, C. Klingshirn, and K. Bohnert, Phys. Rep. **124**, 161 (1985).

[38] D. M. Whittaker *et al.*, Phys. Rev. Lett. **77**, 4792 (1996).

[39] V. Savona, C. Piermarocchi, A. Quattropani, F. Tassone, and P. Schwendimann, Phys. Rev. Lett. **78**, 4470 (1997).

[40] D. M. Whittaker, Phys. Rev. Lett. **80**, 4791 (1998).

[41] C. Ell *et al.*, Phys. Rev. Lett. **80**, 4795 (1998).

[42] R. P. Stanley, S. Pau, U. Oesterle, R. Houdre, and M. Ilegems, Phys. Rev. B **55**, R4867 (1997).

[43] J. Wainstain *et al.*, Solid State Commun. **106**, 711 (1998).

[44] J. Wainstain *et al.*, Superlattices Microstruct. **22**, 389 (1997).

[45] R. P. Stanley (private communication).